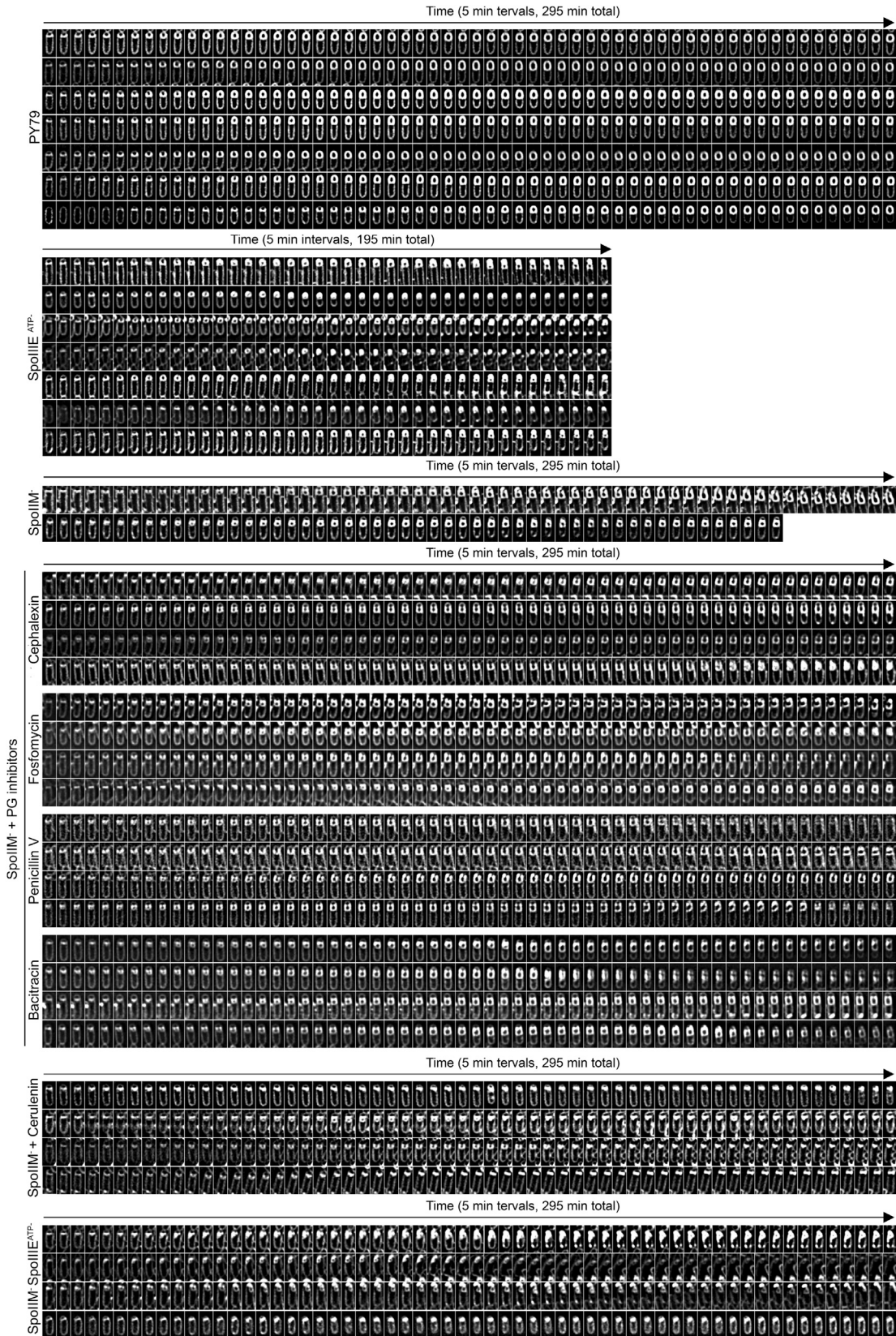


**Figure S1. Forespore Growth over Longer Time, Related to Figure 1**

(A) Timelapse fluorescence microscopy of wild-type sporangia stained with the membrane dye FM4-64. Each row is a different sporangium. The time between two consecutive snapshots is 20 min, and the total time of each series is 4 hours. The asterisk indicates the time point at which engulfment completes.

(B) Change in forespore volume over time, extracted from timelapse movies. For each time point, the average and standard deviation of 41 sporangia is shown. The green vertical band indicates the time interval at which engulfment membrane migration is completed for the analyzed sporangia. The timelapses were aligned so that 0 h was the time immediately before the time point at which the flat sporulation septum started to curve.



---

**Figure S2. Full Timelapse Microscopy Series, Related to Figures 1 and 2**

This figure is provided at high-resolution and zoom-in is recommended for proper visualization. Timelapse microscopy of wild-type sporangia, SpoIIIE<sup>ATP-</sup> sporangia, SpoIIIM<sup>-</sup> sporangia, SpoIIIM<sup>-</sup> sporangia treated with cephalixin (50  $\mu$ g/ml), fosfomycin (6900  $\mu$ g/ml), penicillin V (500  $\mu$ g/ml), bacitracin (50  $\mu$ g/ml) or cerulenin (30  $\mu$ g/ml), and SpoIIIM<sup>-</sup> SpoIIIE<sup>ATP-</sup> sporangia. Images were collected at 30 $^{\circ}$  C every 5 minutes for a total of up to 295 minutes. Each row represents a different sporangium and all the collected time points are shown. Membranes were stained with FM4-64.

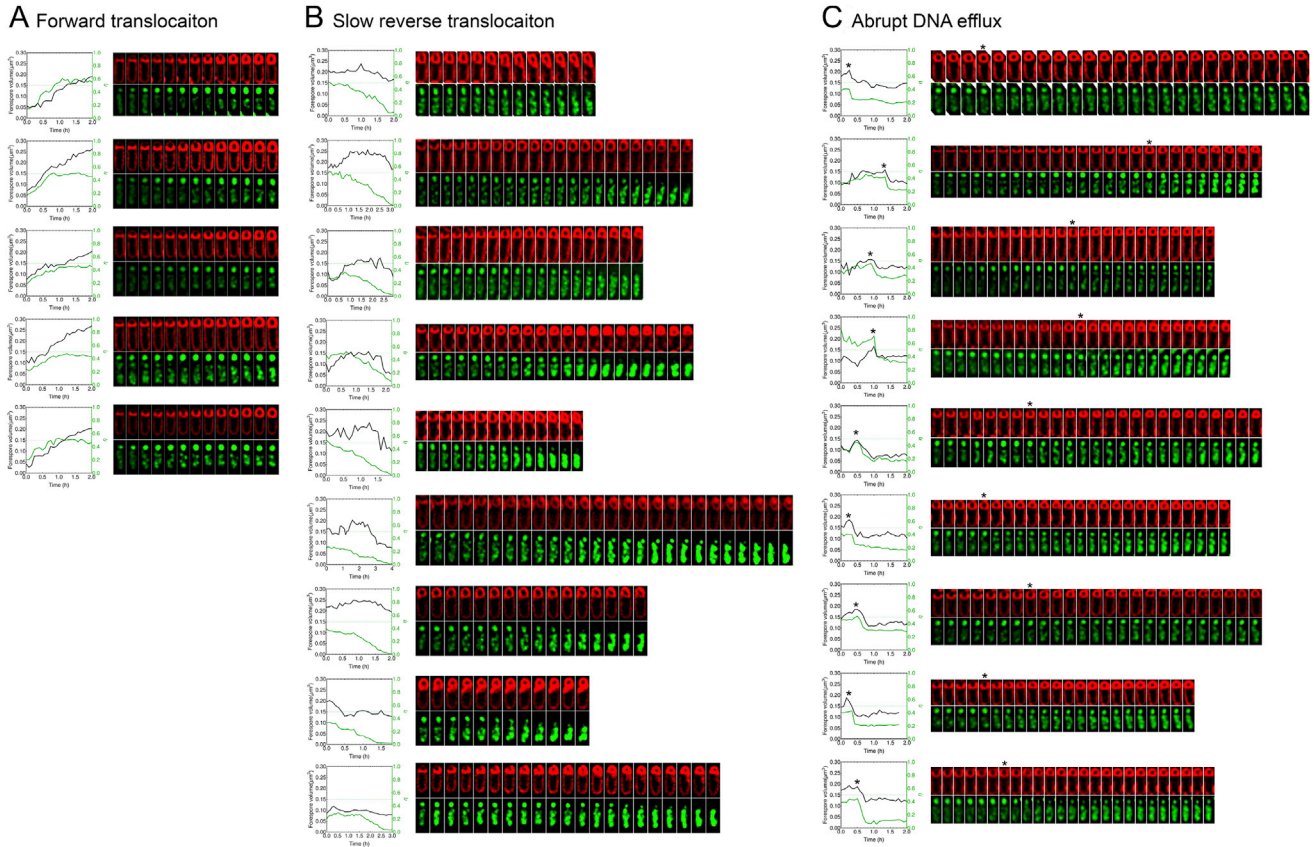


**Figure S3. Forward and Reverse Chromosome Translocation, Related to Figure 3**

This figure is provided at high-resolution and zoom-in is recommended for proper visualization. Examples of control sporangia (A) in which the chromosome is completely translocated from the mother cell to the forespore, and sporangia in which SpoIIIE is degraded in the mother cell (B and C) and the chromosome is slowly (B) or abruptly (C) translocated out of the forespore. Membranes are stained with FM4-64 and DNA with SYTOX green. Snapshots taken every 10 min are shown for (A) and (B), and every 5 min for (C). Graphs show forespore volume (black line, left y axis) and fraction of DNA intensity in the forespore,  $\eta$  (green line, right y axis), over time of the sporangium immediately next to them. The green dotted line represents the fraction DNA intensity in the forespore corresponding to full chromosome translocation. The asterisks in (C) indicate the onset of the chromosome abrupt transport out of the forespore.

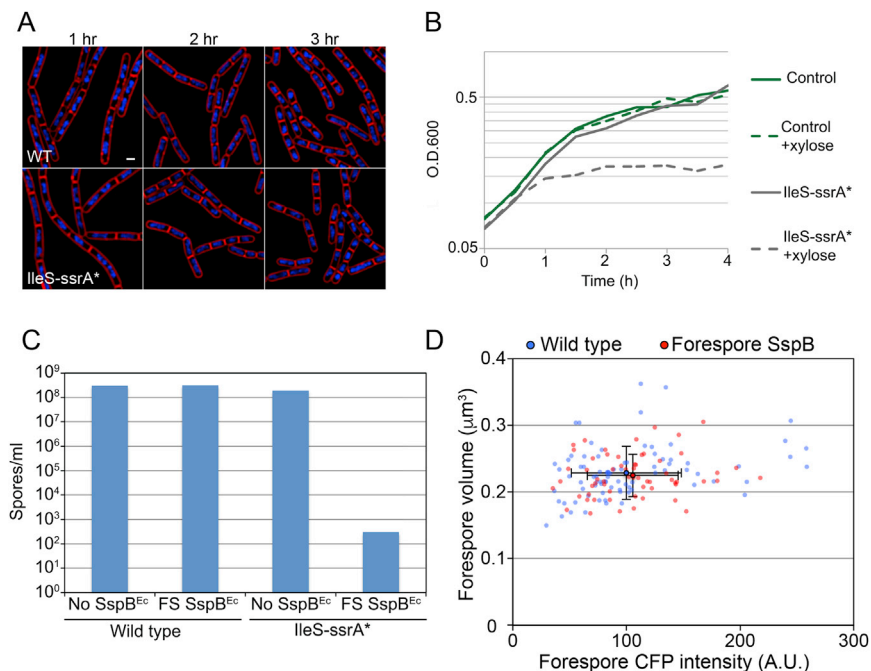


**Figure S4. *IleS-ssrA\** Is Efficiently Degraded and *sspB<sup>Ec</sup>* Expression in the Forespore Does Not Affect Either Translation or Forespore Size, Related to Figure 4**

(A) Fluorescence microscopy of non-sporulating wild-type and *IleS-ssrA\** strains. Membranes were stained with FM4-64 and DNA with DAPI. Scale bar, 1  $\mu\text{m}$ . Images were taken at the indicated time points after diluting a late exponential culture to  $\text{O.D.}_{600} = 0.2$ .

(B) Growth curves of strains producing *SspB<sup>Ec</sup>* under the control of a xylose-dependent promoter ( $P_{xy(A)}$ ), in a background in which *IleS* is not tagged with *ssrA\** (control, green lines), or in a background in which *IleS* is tagged with *ssrA\** (*IleS-ssrA\**, gray lines). Late-exponential cultures of each strain were diluted to  $\text{O.D.}_{600} = 0.2$ , either in the absence of xylose (solid lines) or in the presence of 1% xylose (dotted lines).  $\text{O.D.}_{600}$  measurements were taken every 30 minutes for 4 hours. Production of *SspB<sup>Ec</sup>* in the control does not interfere with growth. However, production of *SspB<sup>Ec</sup>* in the *IleS-ssrA\** background abolishes growth, suggesting that *IleS-ssrA\** is efficiently degraded.

(C) Spore titers of wild-type and *IleS-ssrA\** strains in the absence of *SspB<sup>Ec</sup>* (No *SspB<sup>Ec</sup>*) or when *SspB<sup>Ec</sup>* is produced in the forespore from  $P_{sspE(2G)}$  (FS *SspB<sup>Ec</sup>*). Production of *SspB<sup>Ec</sup>* in the forespore does not interfere with spore formation in wild-type background, but produces a dramatic reduction ( $\sim 10^6$  folds) in spore titers in *IleS-ssrA\** background. The averages of three independent experiments are shown.

(D) Plot representing the total CFP fluorescence intensity in the forespore (x axis) versus forespore volume (y axis) of wild-type sporangia (blue dots), or of sporangia in which *SspB<sup>Ec</sup>* is produced in the forespore, but in which no protein is tagged with *ssrA\** (red dots). Each dot represents an individual forespore. The solid dots represent the average CFP intensity and volume of wild-type sporangia (blue,  $N = 141$ ) and sporangia in which *SspB<sup>Ec</sup>* is produced in the forespore (red,  $N = 61$ ). The error bars represent the standard deviations. No significant differences are observed on the CFP intensity ( $p = 0.4345$ ) or forespore size ( $p = 0.4812$ ) between the two strains.

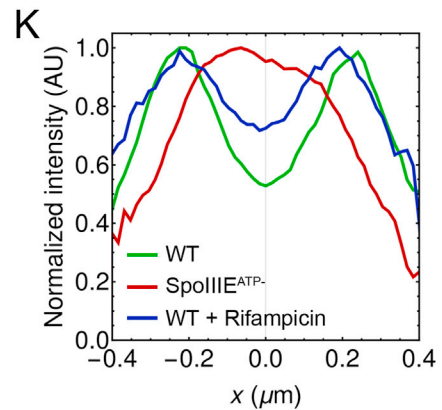
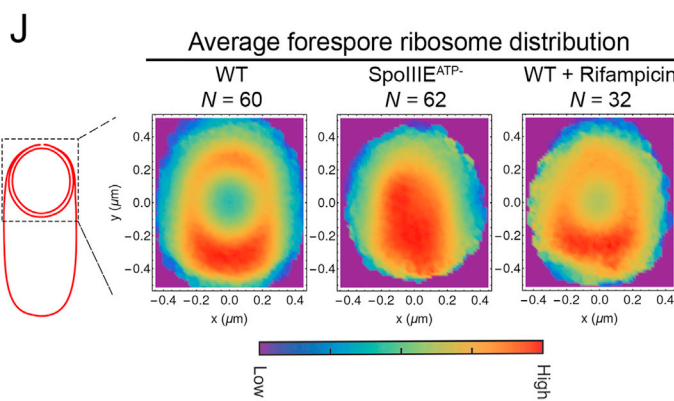
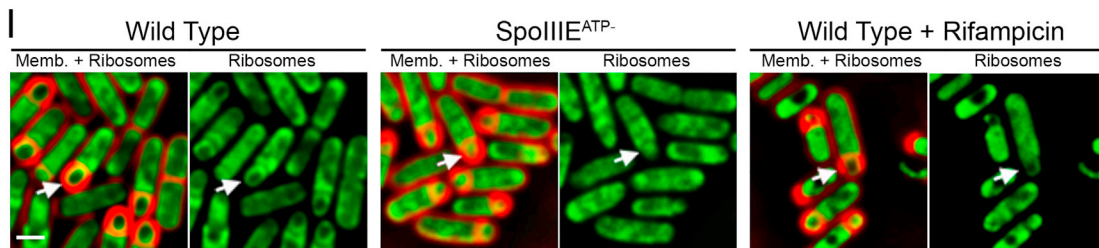
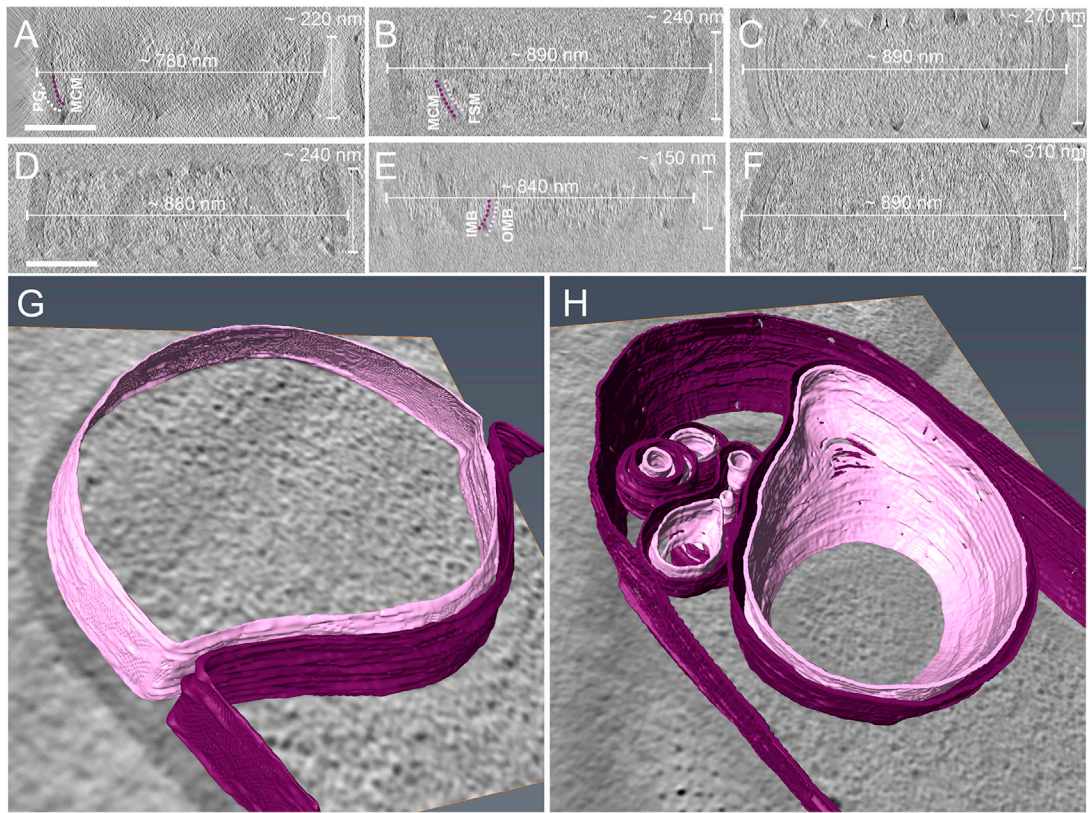


**Figure S5. FIB-CE Tomograms Thickness and Membrane Segmentation, Related to Figure 6**

(A–F) Cells shown in Figure 6A–6F have been rotated 90° around the short axis of the respective cell. The mother cell membrane (MCM) and forespore membrane (FSM) are highlighted with magenta and pink dotted lines, and PG with white dotted lines. Inner membrane of the bleb (IMB) and outer membrane of the bleb (OMB) for the tomogram shown in Figure 6E are highlighted with magenta and pink dotted lines, respectively, in the rotated view in shown in S5E. The thickness of each lamella as well as the approximate width of the plane at which the slice of the tomogram was taken for Figure 6A–6F is shown for each cell. The volumes

(legend continued on next page)

---

enclosed by the milled forespores shown in [Figure 6B](#) (and [B](#)) and [Figure 6E](#) (and [E](#)) are  $\sim 0.062 \mu\text{m}^3$  and  $\sim 0.046 \mu\text{m}^3$ , respectively (measured by segmenting the forespore in Amira), and there are  $\sim 167$  and  $\sim 79$  ribosomes in those volumes. Scale bars, 200 nm.

(G) Segmentations of the forespore and mother cell membranes of the sporangium shown in [Figure 6D](#) (and [S5D](#)) with a wavy appearance.

(H) Segmentations of the forespore and mother cell membranes of the sporangium shown in [Figure 6F](#) (and [S5F](#)). Excess membrane that accumulates at the mother cell distal pole has also been shown. The forespore membrane is shown in pink, the mother cell membrane in magenta. Scale bars have been omitted in panels G and H as a perspective view of the cells is shown.

(I) Fluorescence microscopy of wild-type sporangia (left),  $\text{SpoIIIE}^{\text{ATP}^-}$  sporangia (middle) and wild-type sporangia treated with rifampicin (0.25  $\mu\text{g}/\text{ml}$ ) for one hour (right) to stop transcription, expressing a GFP fusion to the ribosomal protein S2 (encoded by *rpsB*) to visualize ribosome distribution. The concentration of rifampicin used is five times higher than the minimal inhibitory concentration ([Lamsa et al., 2016](#)). The arrows point at representative forespores. Membranes were stained with FM4-64. Scale bar, 1  $\mu\text{m}$ .

(J) Average ribosome distribution in wild-type forespores (WT, right),  $\text{SpoIIIE}^{\text{ATP}^-}$  forespores (middle), and wild-type forespores treated with rifampicin (WT + Rifampicin, left).

(K) Normalized fluorescence intensity along a horizontal line that cross (at  $y = 0$ ) the averaged forespores shown in (J). Fluorescently-labeled ribosomes localize to the forespore periphery in wild-type sporangia, but are homogenously distributed in  $\text{SpoIIIE}^{\text{ATP}^-}$  forespores, in agreement with CET results ([Figure 6G–6J](#)). Ribosomes still tend to localize to the forespore periphery after treatment with rifampicin for one hour, suggesting that the peripheral localization of the ribosomes is not entirely due to the presence of transcriptionally active loops at the forespore periphery. It is likely that the compacted chromosome physically excludes ribosomes due to an excluded volume effect: Forespores are only 0.1–0.2  $\mu\text{m}^3$  in volume (compared to 1  $\mu\text{m}^3$  for mother cells), and we estimate that packing a  $\sim 4$ -megabase chromosome into this small volume will create a DNA mesh with an average pore diameter of  $< 20$  nm (see [STAR Methods](#) for calculation details), significantly smaller than what has been estimated for *E. coli* cells ( $\sim 50$  nm; [Castellana et al., 2016](#)). *Bacillus* ribosomes have a diameter of  $\sim 20$  nm, and therefore would be unable to freely diffuse inside the nucleoid.

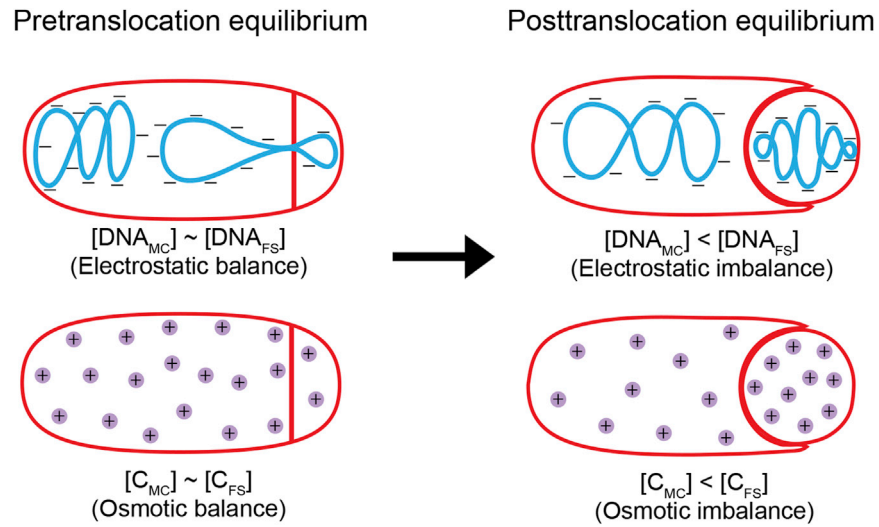


**Figure S6. Gibbs-Donnan Effect to Explain the Osmotic Difference between Mother Cell and Forespore, Related to Figure 7**

Right after polar septation, the forespore and mother cell are in both electrostatic and osmotic equilibrium, as the same concentration of charges and ions are present in both cells. The translocation of the polyanionic chromosome to the forespore generates an electrostatic imbalance, since the concentration of DNA in the forespore is higher than in the mother cell, due to the size difference of both cells. Because the DNA cannot diffuse freely between the forespore and the mother cell, the electrostatic imbalance is compensated by the redistribution of positively-charged ions (purple circles), which become more concentrated in the forespore. In turn, this creates an osmotic difference between both cells, which ultimately results in a net water flow to the forespore, leading to an increase in turgor pressure.



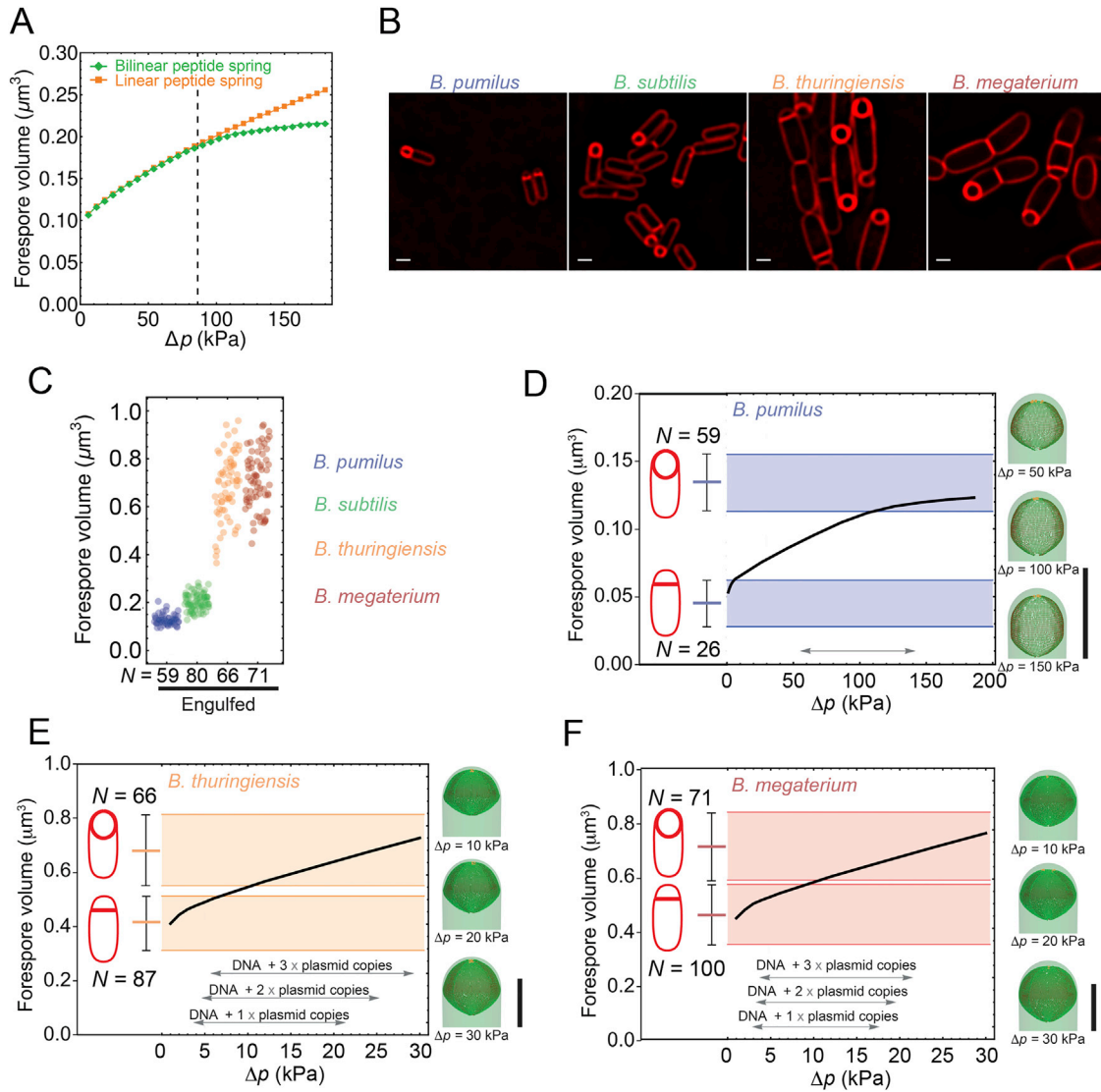


**Figure S7. Simulations for Different Peptide Models and Different *Bacillus* Species, Related to Figure 7**

(A) Forespore volume at the end of engulfment versus pressure difference ( $\Delta p$ ) between forespore and mother cell. Peptides are modeled as linear springs with effective spring constant  $k_{\text{pep}} = 25$  pN/nm, or bilinear peptide springs with effective spring constants  $k_{\text{pep1}} = 25$  pN/nm for peptide elongation up to 50% natural spring length, and  $k_{\text{pep2}} = 1100$  pN/nm for elongations larger than 50% natural spring length (Nguyen et al., 2015; Ojic et al., 2016). Simulations with linear or bilinear peptides show no significant difference up to pressures of  $\sim 100$  kPa. In our simulations we used bilinear spring constants. Vertical line represents maximum pressures used to simulate engulfment in Figure 7.

(B) Fluorescence microscopy images of *B. pumilus*, *B. subtilis*, *B. thuringiensis*, and *B. megaterium* sporulating cultures. Membranes were stained with FM4-64. The scale bars are identical for every species (1  $\mu\text{m}$ ).

(C) Forespore volume of sporangia that completed engulfment membrane migration (engulfed) for different *Bacillus* species: *B. pumilus* (blue), *B. subtilis* (green), *B. thuringiensis* (orange) and *B. megaterium* (red). Each dot represents a different forespore. The number of forespores measured in each set ( $N$ ) is indicated at the bottom of the graph.

(D–F) Simulated forespore volume after engulfment (black lines) for *B. pumilus* (D), *B. thuringiensis* (E) and *B. megaterium* (F) as a function of  $\Delta p$ . *B. subtilis* simulations are shown in Figure 7. The average forespore volume of sporangia that just underwent polar septation (flat septa) and of sporangia that completed engulfment membrane migration (engulfed) is shown on the left side of each graph. The error bars represent the standard deviation, and the number of forespores measured ( $N$ ) is indicated inside the graph. The difference in volume between engulfed and flat septum sporangia provides a rough estimate of how much forespores grow during engulfment. On the right side of each graph, the horizontal bands represent average volume  $\pm$  STD of forespores with flat septa (lower band) and fully engulfed forespores (higher band). Theoretically calculated ranges of osmotic pressures generated by genome packing in the forespore are shown with gray arrow bars at the bottom of the graphs. Chromosome sizes of the different species are provided in the STAR Methods. For *B. thuringiensis*, and *B. megaterium*, which contain large plasmids, theoretically calculated ranges of osmotic pressures are shown taking into account uncertainties in forespore plasmid numbers in the forespore. Simulations show that osmotic pressure due to packing the genome in the forespore is enough to explain forespore growth during engulfment in the different *Bacillus* species. Simulation snapshots for different  $\Delta p$  are shown to the right of each graph. Scale bars, 1  $\mu\text{m}$ .